Eindhoven University of Technology

BACHELOR

Wave making resistance in human swimming

Spee, S.J.H.

Award date:
2018

Link to publication

Disclaimer
This document contains a student thesis (bachelor's or master's), as authored by a student at Eindhoven University of Technology. Student theses are made available in the TU/e repository upon obtaining the required degree. The grade received is not published on the document as presented in the repository. The required complexity or quality of research of student theses may vary by program, and the required minimum study period may vary in duration.

General rights
Copyright and moral rights for the publications made accessible in the public portal are retained by the authors and/or other copyright owners and it is a condition of accessing publications that users recognise and abide by the legal requirements associated with these rights.

- Users may download and print one copy of any publication from the public portal for the purpose of private study or research.
- You may not further distribute the material or use it for any profit-making activity or commercial gain

– Wave making resistance in human swimming –

S.J.H. Spee (0894997)

July, 2018

Bachelor Thesis

Supervisors: Prof. dr. ir G.J.F. van Heijst, J. van Houwelingen

Abstract

The wave drag on a swimmer is analyzed in a towing experiment with two human participants. The swimmer is towed in streamlined position through a swimming pool at constant velocity when holding a buoy with a force sensor. The depth and velocity are varied across different trials. Three interventions are tested at surface level depth. The drag force and coefficients are calculated and considered as a function of velocity, depth and Froude number. Also an estimation of the contributions of wave drag to total drag has been made based on the wave energy. Tests on one subject showed that the drag increased when the depth reaches the surface. Slightly lifting the head and rotating the body 90°along the longitudinal axis both gave an increase in drag. The wave energy per one meter of horizontal area is roughly estimated around 14% of the total energy the swimmer used during the wave period. For further research it is recommended to test more velocity-depth combinations and to use more different swimmers. This would improve the consistency of the research done.

Contents

1 Introduction

During competitive swimming, the goal is to cover a desired distance in the shortest amount of time possible. Research can help swimmers in reaching this goal, for example by finding ways to reduce drag forces counteracting the swimmer's motion or enhance the generation of propulsive forces. In this study, wave drag on the entire swimmer is studied. Hereby the goal is to gain more understanding of the contributions of wave drag to total drag as function of the velocity and depth of the swimmer. It would be interesting to find interventions that affect this wave drag.

In shipping there have been found techniques to reduce this wave drag, like the bulbous bow [1], but also some animals like ducklings have found ways to limit the influence of wave drag [2]. Ducklings use lift to raise the body above the water surface, whereby the influence of wave drag is avoided. In swimming, wave drag appears to have a high impact. Although, there is some inconsistency between previous studies who studied this influence of wave drag. Contributions ranging between $50-60\%$ [3] and 5% [4] have been proposed. This inconsistency raises questions that require more research.

For this study, an experiment is done the training pool of the Pieter van den Hoogenband Stadium at the Innosportlab in Eindhoven. The experiment is done by towing a human swimmer through a swimming pool at different depths and velocities and measuring the force that is necessary to tow the swimmer at constant speed.

To get a better understanding of the physics behind the experiment, theory about drag in general and wave drag specific is explained in more detail in section 2. Also some explanation about vortex shedding is given. Section 3 describes the experimental setup and method for during both the experiment and analysis. Section 4 gives the final results and this will be followed up by a discussion and final conclusion.

2 Theory

In this section, the theoretical concepts related to the towing experiment are reviewed. In the first part of this section, all drag forces on a swimmer are reviewed. In the second part, wave drag is explained in more detail. The final part of this section gives some information about vortex shedding.

2.1 Drag in human swimming

During swimming, the swimmer experiences a lot of drag forces that work opposite to motions of the swimmer. A simplified schematic overview of all forces that are experienced during swimming is given in figure 2.1. When studying the forces on a swimmer a distinction is made between passive drag and active drag. The drag experienced by a swimmer in a passive position is referred to as passive drag. The total drag while actively propelling is called active drag[5].

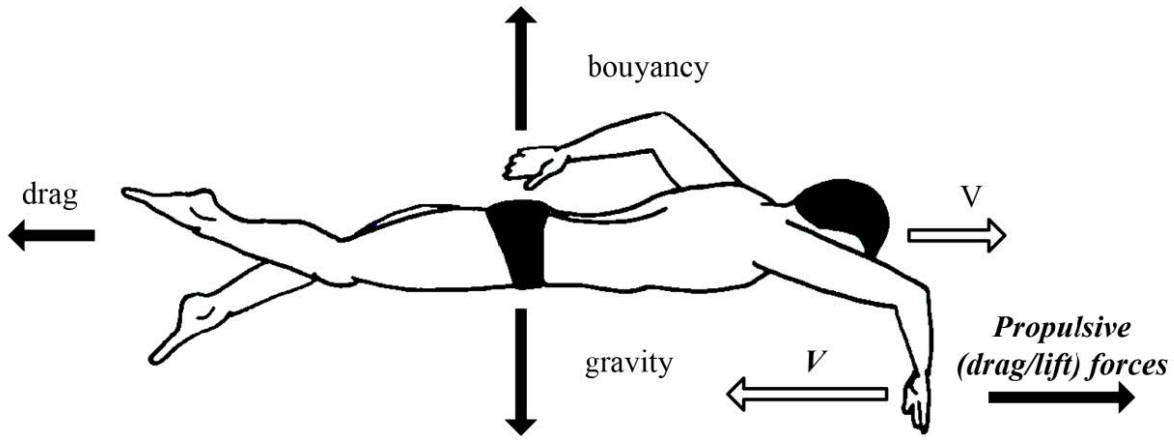

Figure 2.1: Schematic overview of the forces on the entire swimmer [6]

The hydrodynamic drag can be separated into three major components: frictional drag, form or pressure drag and wave drag. Frictional drag represents the component of drag that is due to viscous friction between the water and body surface of the swimmer. Form or pressure drag is dependent on the form of the body and due to pressure difference between the frontal surface and the rest of the body[7]. Wave drag will be explained in section 2.2.

A generalized expression for the total drag force $\vec{F}_D$ that a body experiences having a certain velocity V is:

$$\vec{F}_D = \frac{1}{2} C_D \rho A V^2 \hat{v}, \tag{2.1}$$

with ρ as the density of the medium, A the surface projected on a plane perpendicular to the mean flow and C_D as the dimensionless drag coefficient. In this study A is the frontal surface of the swimmer in streamlined position. The drag coefficient is a dimensionless quantity, which is unique for every object and includes all drag components that are mentioned above. C_D depends on the Reynolds number, that represents the ratio between inertia and viscous forces and is expressed as:

$$Re = \frac{VL}{\nu}, \tag{2.2}$$

where V is the typical velocity, L the typical length, and ν the kinematic viscosity of the fluid.

2.2 Wave drag

When a swimmer moves through the water around surface level, waves are produced. The energy of these waves have to be provided by the swimmer's power, since this is the only source that can account for this additional energy. The swimmer experiences this as a drag force, usually refered to as wave drag[3].

In a previous study on mannequins towed through the water, it is found that wave drag has a large contribution to the total passive drag [3]. The results of this study are shown in figure 2.2. The fits show a clear difference between the drag when towed around the surface and when being fully immersed. The increase in drag as function of velocity is higher for mannequins towed around the surface levels compared to fully immersed mannequins. Since in this study the wave drag is assumed to be minimal when the mannequin was fully immersed and to be independent of skin and form drag, the difference between these drag curves is due to wave drag. This difference is illustrated with the dashed curve in figure 2.2 [3].

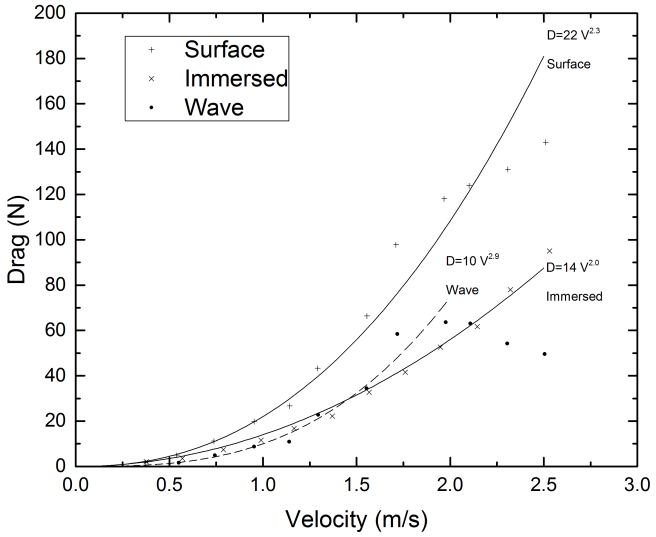

Figure 2.2: Power law fit of passive drag at the surface, fully immersed and wave drag as function of velocity.[3]

Wave drag is depends on the Froude number, which is the ratio between stationary inertial forces and the gravitational force, expressed by:

$$Fr = \frac{V}{\sqrt{gL}}, \tag{2.3}$$

with g as the gravitational acceleration [8].

2.2.1 Hull speed

When the velocity V of an object (for example a swimmer or a boat) traveling through the water surface increases, the wavelength λ of the bow wave also increases [2]. This is illustrated in figure 2.3 a to c. At some point, the boat reaches a critical velocity where the wave length λ equals the hull length L. This critical velocity is called the hull speed V_{hull}, given by [2]:

$$v_{hull} = \sqrt{\frac{g}{2\pi}}\sqrt{L} \approx 1.25\sqrt{L}. \tag{2.4}$$

The Froude number (2.3) calculated for hull speed (2.4), amount to $Fr \approx 0.4$. When an object reaches hull speed, the generated bow wave limits a further increase of velocity because the object has to climb up its own bow wave. This corresponds with a drastic increases of wave drag and thus it costs a lot more power to reach and maintain some velocity.

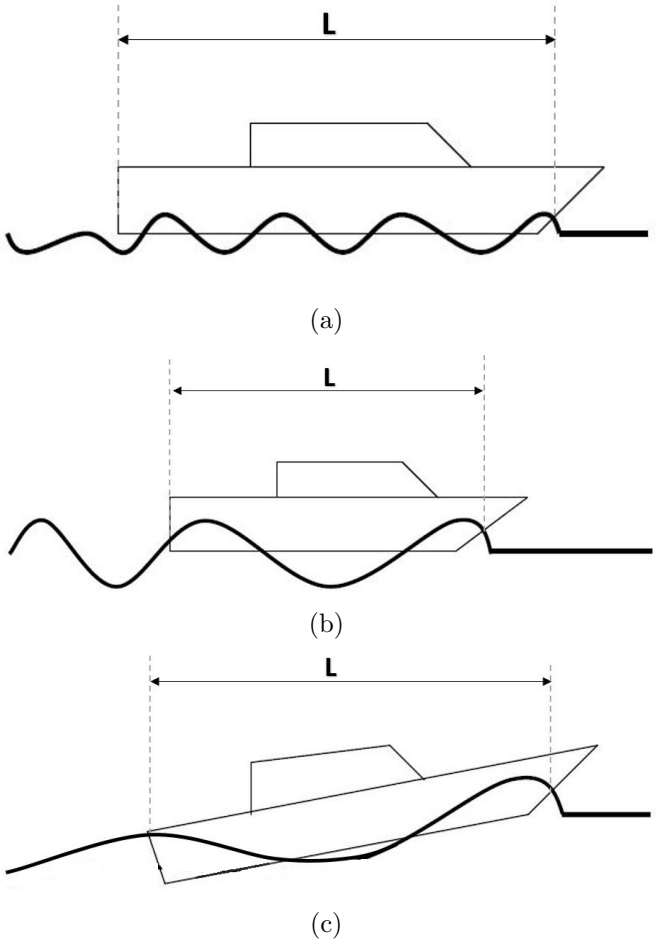

Figure 2.3: Two-dimensional illustration of wake wave relative to hull length in the different situations: (a) below hull speed; (b) at hull speed; (c) exceeding hull speed

Nevertheless, there are ways to avoid the large wave drag at speeds higher than hull speed. Boats for example can make use of generated hydrodynamic lift as it rises to a planing condition [3]. Young ducklings make use of lift to raise the body above the water surface whereby they appeared to be able to reach a maximum burst speed that is four times greater than predicted hull speed based on body lengths [2].

2.2.2 Wave energy

Since this study is performed in the swimming pool of 1.9 m deep, the deep-water limit applies. In the deep-water limit the length of the waves are much smaller than the depth of the pool and thus it holds that:

$$\frac{2\pi H}{\lambda} > 1.75, \tag{2.5}$$

with H as the depth and λ as the wavelength [9]. The phase velocity v_p in the deep-water limit can be approximated by:

$$v_p = \sqrt{\frac{g\lambda}{2\pi}} \tag{2.6}$$

and group velocity v_g becomes half the phase velocity [9]:

$$v_g = \frac{1}{2}v_p. \tag{2.7}$$

There exists some disagreement about the contribution of wave drag in the total drag of a swimmer. Vennell et al. (2006) found a 50−60% contribution of wave drag at a speed of 1.7 m/s, while Vorontsov and Rumyantsev (2000) state that 5% of total drag is due to wave drag at a speed of 2.0 m/s. All these studies concerning wave drag in swimming gave their result in terms of drag force. An alternative method to tackle this problem might be the determination of the energy contained in the produced wave. The wave energy is reflected in the potential E_{pot} and kinetic energy E_{kin} of a wave. Generally, the energy E_{wave} per unit horizontal area of free-surface wave is represented as:

$$E_{wave} = E_{kin} + E_{pot} = \frac{1}{2}\rho g a^2, \tag{2.8}$$

with ρ as the density of the fluid and a as the amplitude of the wave [9]. To find the total wave energy, E_{wave} has to be multiplied with a certain length. Since a swimmer does not produce a uniform wave in one direction, the determination of this desired length and with that calculating the total wave energy is difficult. The total energy can be illustrated by the work that is done to move the swimmer and is given by:

$$E = F_D s = F_D V T, \tag{2.9}$$

with s as the distance traveled during one period T of the produced wave and V as the velocity of the swimmer.

2.3 Frequency analysis

The measured drag force on a body is typically not constant over time. Vortex shedding from the body results in fluctuating forces. For a large range of Reynolds numbers, these fluctuating forces result in periodic vortex shedding that repeats itself with a certain frequency f. This repeating pattern is called a Von Kármán vortex street [8]. In figure 2.4 the von Kármán street of a cylinder at $Re = 55$ is shown as an example. A useful measure to characterize the vortex shedding frequency f is the Strouhal number. The Strouhal number is defined as the ratio between non-stationary and stationary inertial forces and given by:

$$St = \frac{fL}{V}, \tag{2.10}$$

with characteristic length L and flow velocity V. Experiments with cylinders show that for a large range of Re numbers, St remains close to 0.21 [8, 10]. Although the Strouhal number is in swimming research often used as an important property to characterize stroke frequencies [11], no literature is found to the relation of the Strouhal number based on vortex shedding. The body geometry of a swimmer is complex, which might result in a variety of vortex shedding frequencies in the wake. To obtain typical frequencies of the fluctuating force data a Fourier analysis can be used. This method transforms the time domain into a frequency domain.

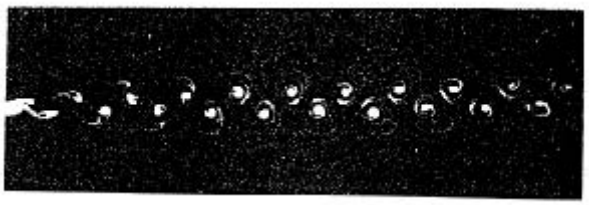

Figure 2.4: Von Kármán vortex street behind a cylinder at Re = 55 [8]

3 Experimental set-up

3.1 Setup

The setup of the towing experiment is shown in figure 3.1. Relevant parameters are indicated in the figure. The experiment is conducted in the indoor training pool of the Pieter van den Hoogenband swimming stadium at Innosportlab in Eindhoven, the Netherlands. The pool measures 50 m in length, 10 m in width and 1.9 m in depth. Two experienced swimmers that are competing on the national level participated voluntarily and gave their written informed consent. In table 1, the relevant physical characteristics of the swimmers are given. The swimmers wore a swimming trunk on which a LED is attached on the right hip. An electromotor mounted on the starting platform pulls the rope with a prescribed constant speed. The force measurement is performed with a dynamometer in a bouy that is attached at end of the rope. The force sensor is connected with a seperate cable for data transfer to a computer. During the measurements, the swimmer holds the buoy and is pulled towards the starting platform by the electromotor. The force that is used to pull the swimmer is recorded as a function of time, with a sample rate of 100 frames per second. The starting position is around 45 m from the starting platform and the towing stopped when the swimmer was around 10 m from the starting platform. The depth d at which the rope is pulled in can be set by adjusting the frame that is mounted on the starting block.

Table 1: Physical characteristics of human subjects

	Normal length (m)	Length in streamlining position (m)	Shoulder width streamlining position (m)	Frontal surface (m^2)
Subject A	1.93	2.46	0.40	0.21
Subject B	1.91	2.47	0.48	0.32

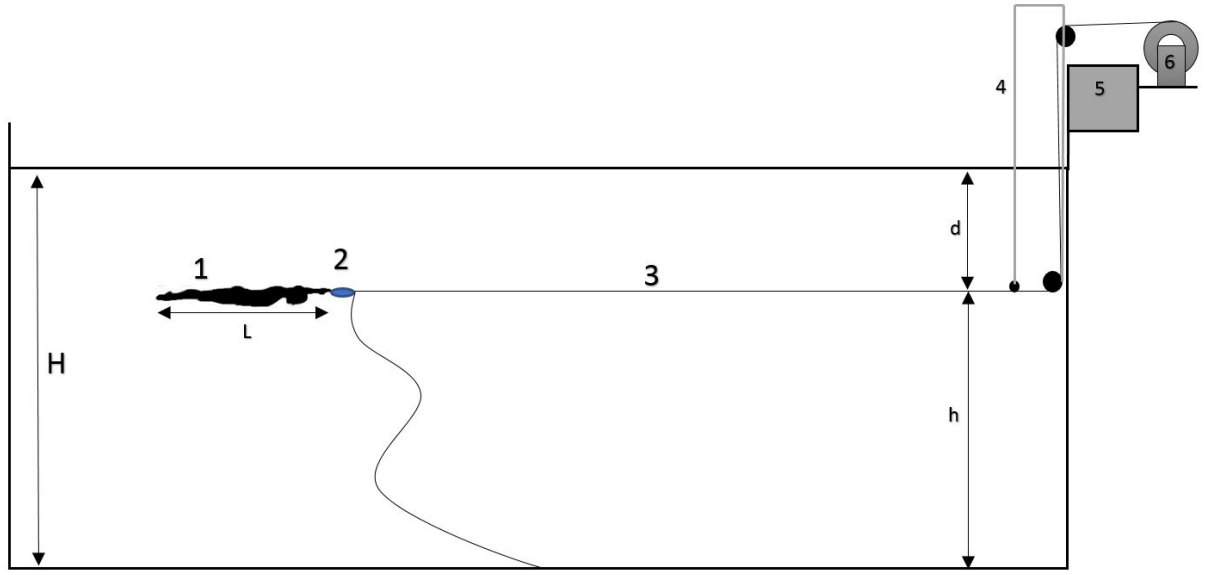

Figure 3.1: 2D schematic of the setup; 1: swimmer, 2: dynamo-meter, 3: towing rope, 4: iron frame with pulleys that can be adjusted to set the depth, 5: starting platform, 6: electric motor

To keep track of the height and velocity of the swimmer, the motion of the swimmer is recorded by Basler SC1400gc cameras that are installed in the 50 m wall on the right for the swimmer. The cameras that are used for this experiment are positioned at 25 and 30 m. A description of this method is given in section 3.1.2.

3.1.1 Calibration

To calibrate the dynamometer and to convert the force signal in Volts (V) to Newtons (N), different measured weights are attached to the dynamometer next to the pool and the data is recorded for a couple of seconds per weight. A linear fit for the force as a function of the voltage is determined with a least square method. The fit and indicated standard deviation is shown in figure 3.2. The equation corresponding to this fit is given by:

$$F = 73.64V - (76.95 \pm 1.14). \tag{3.1}$$

It appears that the fitted curve corresponds well with the measured values.

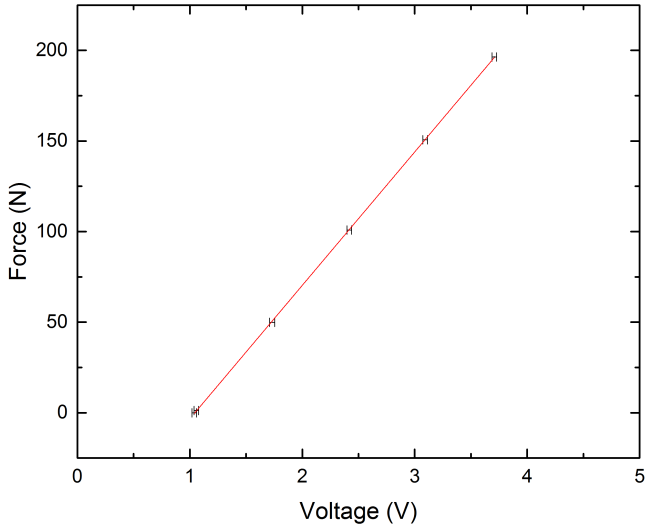

Figure 3.2: Force in newton plotted as a function of force in voltage measured by the force sensor with a linear fit through the data points

3.1.2 Height and velocity check

Two cameras are used to record the height and speed of the swimmer during the trials in order to verify whether it matches the intended height and speed. These data are translated from pixel to world coordinates using a calibration. The calibration is performed afterwards by selecting a set of known coordinates in the record and couple these to pixel coordinates. Subsequently, a polynomial fit is derived through these coupled sets of coordinates. A random pixel coordinate can be converted to world coordinates, when the distance between between the wall with camera and the lane of the swimmer is known. A Matlab script tracks the LED on the

hip of the swimmer frame by frame automatically to capture the instantaneous position and velocity [12].

To check whether the velocity and height of the swimmer is consistent with the desired height and velocity, these are determined with the camera recordings for every trial and averaged per height and velocity. The averaged height, as determined from the video recordings, compared to the aimed height for the trials is shown in table 2. The averaged velocity, as determined from the video recordings, compared to the set velocity of the electromotor is shown in table 3. Trials that do not meet the desired height within a range of ±0.1 m or ±0.1 m/s, are not included in the final results on that height or velocity.

Table 2: The averaged height, as determined from the video recordings, compared to the aimed height for the trials of subject A and B.

Desired height (m)	Determined height (m)	
	Subject A	Subject B
1.9	1.71	1.74
1.6	1.61	1.63
1.0	1.05	1.04

Table 3: The averaged velocity, as determined from the video recordings, compared to the set velocity of the electromotor.

Desired velocity (m/s)	Determined velocity (m/s)	
	Subject A	Subject B
1.0	1.00	0.99
1.5	1.50	1.52
1.7	1.68	1.70
2.0	1.99	2.01
3.0	2.92	2.91

The tables show consistency in the height and velocity measurements, since these measurements are done with the same calibration settings. Especially, the measurements at the water surface shows a large deviation. This is explained by the positioning of the swimmer. The head is at the water surface. However, the legs and hip with the LED are lowered.

3.2 Method

Before the experiment, both swimmers are instructed to remain in streamlining position and to try to keep the same height during the whole run. The experiment is conducted with three different depths d, and five different velocities V. In table 4 the complete list of trials is shown, with all depth-velocity combinations. Some runs have been performed twice to test the consistency of the experiment and setup. Two interventions have been tested at $d = 0.0$ m at velocities 1.7 and 2.0 m/s to analyze the effect on the drag force. The first intervention is with the body rotated 90° along the longitudinal axis of the body, the second intervention is lifting the head slightly. In a third intervention at 2.0 m/s, the swimmer was asked to kick to analyze the effect of kicking on the net drag force.

From the data of the dynamometer, a time frame was selected for further analysis. The average voltage and standard deviation are calculated from this data set. For each trial this value is translated to force by (3.1) and plotted against the velocity. To calculate drag coefficient C_D with (2.1), the frontal surface A is determined. This has been done with the help of Matlab. First the pixel size of the frontal surface during glide is determined from the record of the frontal surface of the swimmer, as shown in figure 3.3. This is converted to a surface in m^2 by calculating the ratio between the shoulder width in m and pixels. The found frontal area A

Table 4: List of trials with all depth-velocity combinations

Depth	Velocity	Intervention
0.9 m	1.5 m/s	
	1.7 m/s	
	1.7 m/s	
	2.0 m/s	
0.3 m	1.5 m/s	
	1.7 m/s	
	2.0 m/s	
0.0 m	1.0 m/s	
	1.5 m/s	
	1.7 m/s	
	1.7 m/s	
	1.7 m/s	Sideways
	1.7 m/s	Slight lift of head
	2.0 m/s	
	2.0 m/s	Sideways
	2.0 m/s	Slight of head
	2.0 m/s	With dolphin kicks
	3.0 m/s	

for each subject is shown in table 1. To account for some inter-individual differences and to normalize the results, the calculated drag coefficient is plotted against as the Froude number Fr as defined by (2.3). All the runs are checked by analyzing the images on height and velocity. If the runs don't verify the desired height within a range of ± 0.1 m or ± 0.1 m/s, they are not included in the final results on that height or velocity.

Figure 3.3: Picture of frontal surface of participant

A Fourier analysis has been performed on the data as a function of time. An attempt has been made to find typical vortex shedding frequencies originating from the body of the swimmer to find relevant frequencies in the spectral domain of the force. By assuming the Strouhal number

of vortex shedding has a value around 0.21, characteristic length scales can be estimated with (2.10), based on the strong frequency components in the spectrum.

Finally, an attempt has been made to an estimate the wave energy. For this estimation, (2.8) has been used. Since it is difficult to determine the described length as stated in section 2.2.2, a length of 1 m is chosen. This energy is compared with the total energy and the found ratio is compared with earlier literature.

4 Results

This section is divided in two parts. Firstly, the total drag and drag coefficient are plotted as described in section 3.2. Secondly, the Fourier analysis is discussed. Finally, the ratio of potential energy by waves and the total energy is estimated.

A typical signal of the dynamometer during a trial is given in figure 4.1. A peak is visible during the first seconds. Since this peak is due to starting effects, this is not taken into further analysis. The dashed lines indicate the data selection that has been used to obtain an average force for each trial.

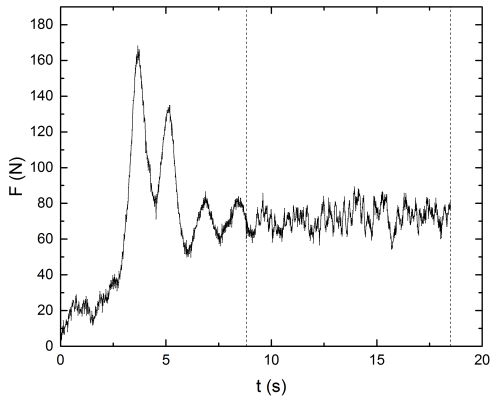

Figure 4.1: Typical data obtained with the dynamometer for the trial at $d = 0.0$ m and $V = 1.7$ m/s (subject A). The force (N) is plotted against the time (s)

4.1 Drag

In figure 4.2 the averaged force data as a function of the velocity is shown for both subjects. Different depths are indicated with different colors. The drag force increases with velocity, as expected from (2.1) that is illustrated by the quadratic fit through the data of trials at 0.0 m in the plot of subject A. A zoomed-in view on the velocities $V = 1.5$, 1.7 and 2.0 m/s is given in figure 4.3. In this figure, the Froude number (eq.(2.3)) is also added to the horizontal axis. The Froude number is calculated based on the finger-to-toe-length when in streamlining position. For subject A it is observed that drag increases when the depth of the swimmer decreases. For subject B no such relation can be observed.

Similar plots were obtained for the drag coefficient as a function of Froude number. These plots are shown in figure 4.4. Drag coefficient C_D is calculated with (2.1), using the fluid density of water at 27.0 C°($\rho = 0.997 \times 10^3$ kg/m^3) and the determined frontal surface areas. It has been noticed that the obtained C_D values for subject B are significantly lower than those for subject A.

The averaged force from the data of trials with the different interventions is plotted against the velocity in figure 4.5. Different interventions are indicated with different colors. It is noticed that for the first two interventions, sideways and slightly lifting the head, the drag is higher

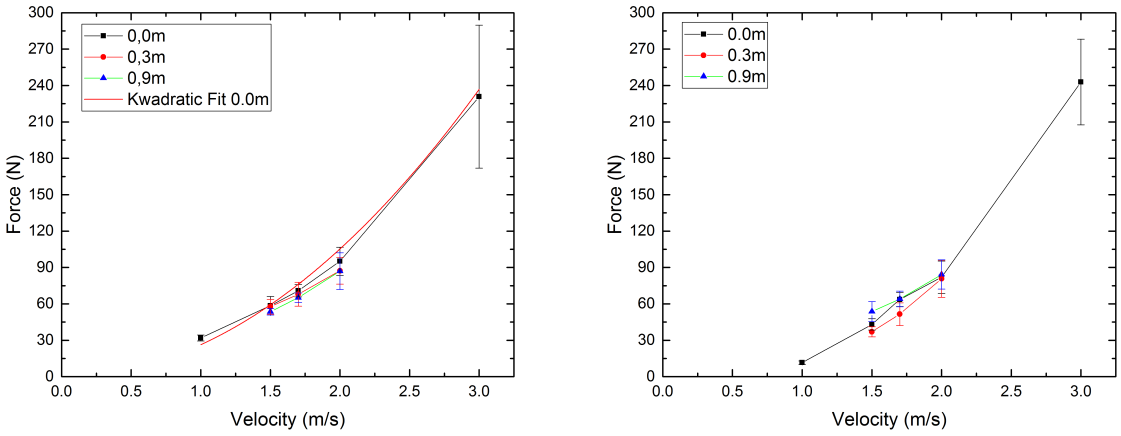

(a) Subject A

(b) Subject B

Figure 4.2: Plots of averaged force against velocity for different depths for the individual swimmers with fit through data of subject A at $d = 0.0$ m.

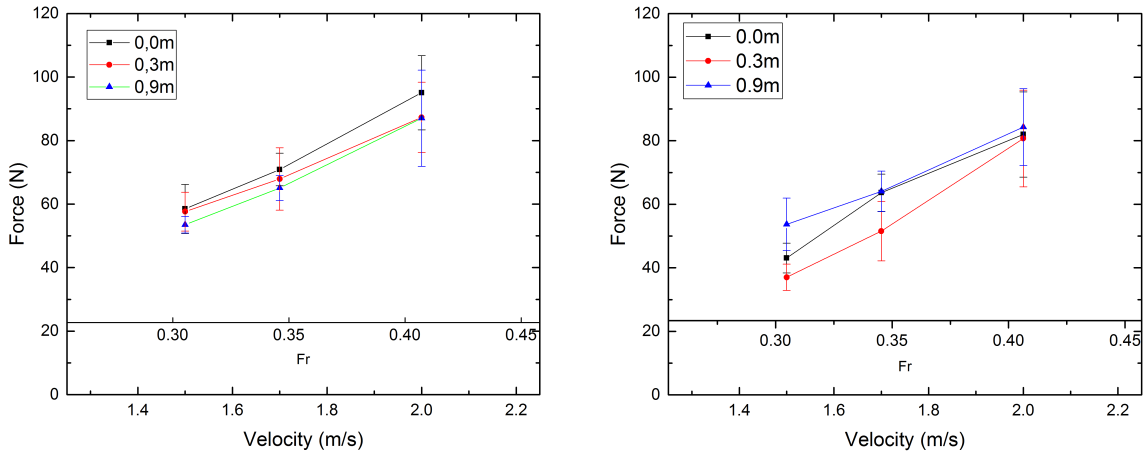

(a) Subject A

(b) Subject B

Figure 4.3: The averaged drag force as a function of velocity and Fr. The results are zoomed-in on velocities 1.5, 1.7 and 2.0 m/s.

relative to the normal position. Kicking while towed had an increasing effect on drag for subject A, but no clear effect on swimmer B.

4.2 Fourier analysis

The measured data are not constant over time, which can be related to vortex shedding. The frequency f is obtained by applying a fast Fourier transform on the data of every trial. A typical spectrum is shown in figure 4.6. By assuming the Strouhal number has a value $St = 0.21$, the characteristic length relating to vortex shedding is calculated by (2.10). From this analysis it

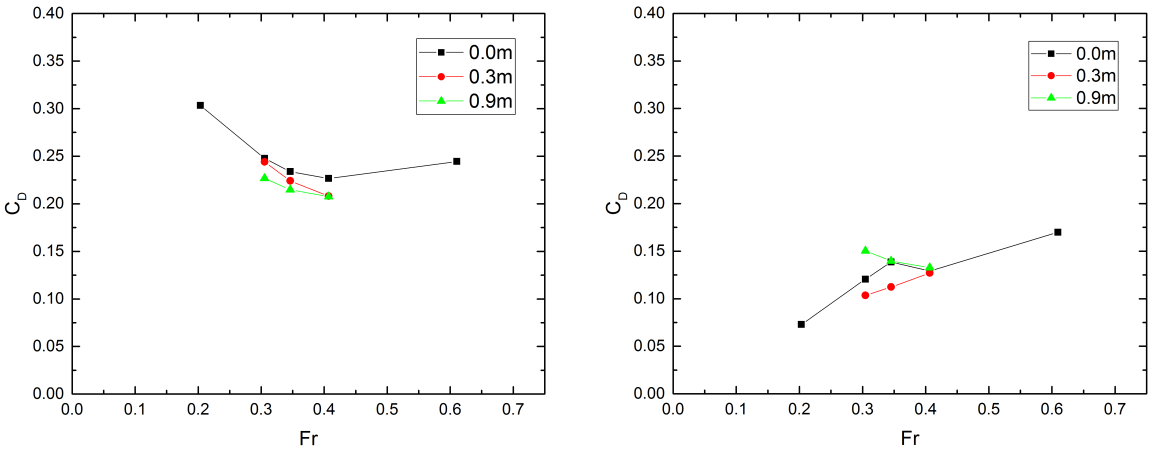

(a) Subject A (b) Subject B

Figure 4.4: Drag coefficient C_D plotted as a function of the Froude number Fr for the individual swimmers

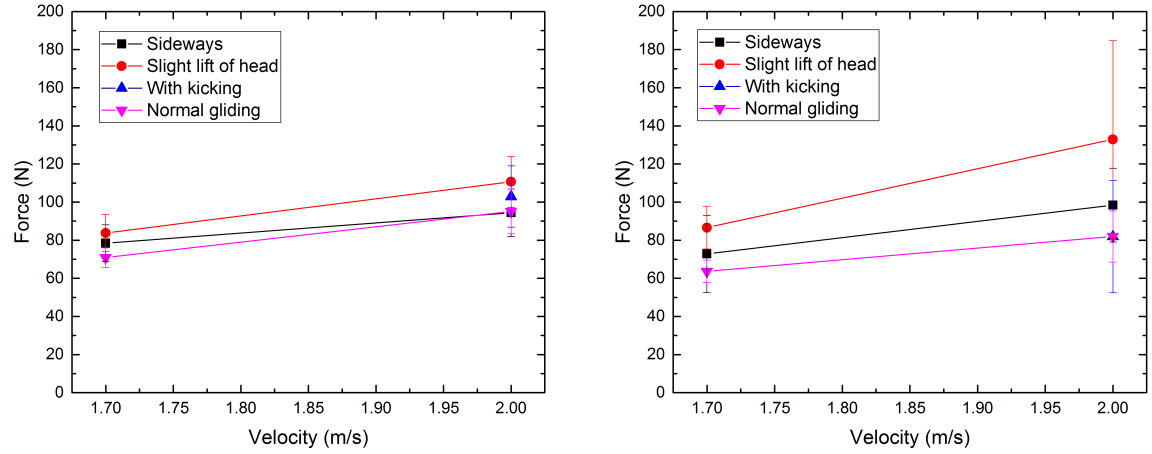

(a) Subject A (b) Subject B

Figure 4.5: Drag force F_D plotted as a function of the velocity V for the different interventions per swimmer

appeared that a large range of different lengths follows from the most dominant frequencies that are visible in the spectrum. The most frequently obtained lengths vary from 1.5 m to 3.5 m. The total range was from 1.5 m to 7 m.

4.3 Wave energy

Additionally, an attempt has been made to calculate the wave energy using eq. (2.8) and based on the observed wave amplitude a. Note that (2.8) is derived under the assumption that the wave made by the swimmer can be obtained as a wave in one direction. In a first approximation,

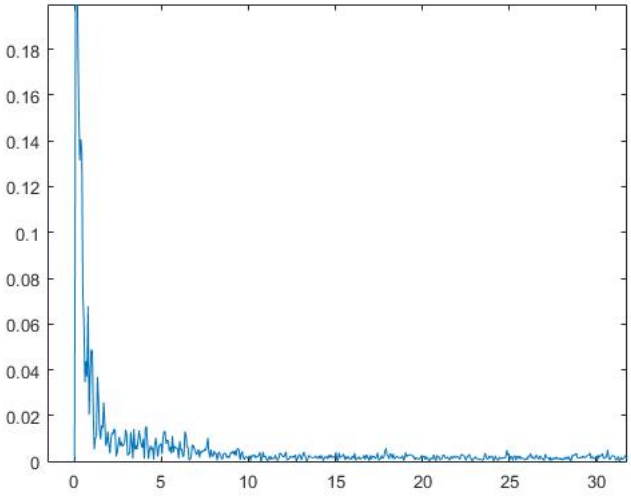

Figure 4.6: Typical spectrum of Fourier transform of the force F measured by the force sensor during the trial at velocity $V = 2.0$ m/s and depth $d = 0.0$ m.

the horizontal distance is set to 1 m. Clear wave formation was visible at trials when towed at the surface with minimal velocity V 1.7 m/s. For this estimation the trial was selected where the clearest wave formation was visible. This is for $V = 3.0$ m/s, where a is estimated around 10 cm. The wave energy E_{wave} for 1 m of horizontal area corresponding to a wave with amplitude $a = 10$ cm is 50 J. The total energy that the swimmer has used during the formation of one wave is calculated by eq. (2.9). The wave period T is determined by using recordings in which the wave shadow is visible. The pixel intensity of a selected pixel is plotted as a function of time, from which the wave period can be distinguished. At $V = 3.0$ m/s the wave period T is around 0.5 s. The work performed to pull the entire swimmer through the water during one wave period is 345 Nm (eq. (2.9)). The ratio between E_{wave} and E, thus the contribution of one meter of horizontal area of wave energy is estimated around 14%.

5 Discussion

The force values per trial obtained by averaging the selected data are in a realistic range of values. This is consistent with previous studies. In section 4.1 it was expected to find a quadratic relation between force and velocity, since equation (2.1) describes this relation. Such quadratic relationship is found for subject A by fitting the data. For subject A it is observed that drag force increases when the body of the swimmer is closer to the water surface, which agrees with the expectation developed by earlier studies. For subject B no such relation was observed. This can be related to more variations in the position of subject B compared to subject A. This type of experiment, with human participants, always includes intra-individual differences. This requires a statistical analysis of a larger number of participants to find whether the results are significant. The differences in drag at the higher velocities that are also tested in this study between different depths were much bigger in Vennell et al. (2006) compared to the data of this study. Compared to the 50-60% contribution of wave drag at 1.7 m/s found in Vennell et al. (2006), this study found a contribution around 8% for subject A at this velocity. This could be due to the use of real swimmers instead of mannequins during the towing experiment. Mannequins have a fixed body position, while human bodies show small changes in streamlined position. Vennell et al. (2006) argues that preliminary tow tests using a human subject showed that small changes in streamlined body posture altered drag around 10% and that human subjects found it difficult to consistently adopt the same streamlined body alignment for all trials near the surface. In our camera images it is clearly visible that the swimmers make small changes in body positioning during the tows. This is probably due to adjustments made by the swimmer to keep the same depth while being towed. In future research to this subject, it is suggested to test more velocity-depth combinations and to use more swimmers. This would increase the consistency of the study.

Since the differences in total drag force between depths are smaller than in earlier studies, this also appeared in the drag coefficient C_D as shown in figure 4.4. Remarkably, between the two subjects there is a clear difference in C_D values. This could be caused by uncertainty in determining the frontal surface A. The frontal pictures of the swimmers in streamlining position contain some perspective that could have caused deviations.

To investigate how different interventions would affect the drag force, thee interventions were tested. The first two interventions, rotated 90° around longitudinal axis and lifting the head slightly, give the same results for both subjects. Lifting the head gives the highest increase in drag and also the 90° rotation increases drag. Applying dolphin kicks did not meet expectation. It was expected that kicking the legs would produce a propulsive drag force and with that reduce the force needed to tow the swimmer. The total drag force on subject B did not change and the drag force on subject A even increased by kicking the legs. A possible explanation of this could be an increased instability of the body when kicking.

The characteristic lengths found by the Fourier analysis differed from 1.5 to 7 m, with most frequencies between 1.5 and 3.5 m. The length scales found with the frequency analysis cannot be directly related to length scales of the body. Lengths that are smaller than the finger-to-toe length of the swimmer might originate from the human body or parts of the human body. However, the dominant frequencies that are larger than this length have to originate from another part of the setup. Maybe the assumption of St ≈ 0.2 is too simple with regard to the entire swimmer, because the swimmer has a complex geometry.

The estimation of the wave energy gives an idea about the share of wave drag in total drag when at surface level. The assumptions used to obtain the wave energy equation are most probably

not valid in this study. The waves produced by the swimmer diverge in different directions, while eq. (2.8) applies to waves that propagate in one direction. This will effect the wave energy. Nevertheless, the approximation of one meter of horizontal area gives the knowledge that the total wave energy around the swimmer will probably be estimated greater than the obtained 50 J. Also the amplitude of the wave could be different than the estimated 10 cm and this could change the ratio a lot.

6 Conclusion

In this experiment, wave drag is analyzed by towing a swimmer through a swimming pool at different depths and velocities. The order of magnitude of the drag force appeared to be consistent with earlier similar experiments. For one subject it is observed that drag increases when the depth of the swimmer decreases. Three different interventions were tested to see how these would affect the drag force. Slightly lifting the head to possibly induce a planing effect gave an increase in drag force. Rotating the body 90° along the longitudinal axis appeared to also have an increasing effect on drag. The share of wave energy of one meter of horizontal area of the total energy of the swimmer was estimated around 14% in a 2D approximation. For further research it is recommended to test more velocity-depth combinations and to use more different swimmers. In this way, the statistical relevance of the results can be obtained.

References

[1] S. Mahmood and D. Huang. Computational fluid dynamics based bulbous bow optimization using a genetic algorithm. *Journal of Marine Science and Application*, 11(3):286–294, 2012. ISSN 1993-5048. doi: 10.1007/s11804-012-1134-1.

[2] T. Aigeldinger and F. Fish. Hydroplaning by ducklings: overcoming limitations to swimming at the water surface. *Journal of Experimental Biology*, 198(7):1567–1574, 1995. ISSN 0022-0949. URL `http://jeb.biologists.org/content/198/7/1567`.

[3] R. Vennell, D. Pease, and B. Wilson. Wave drag on human swimmers. *Journal of Biomechanics*, 39(4):664–671, 2006. doi: 10.1016/j.jbiomech.2005.01.023.

[4] A. Vorontsov and V. Rumyantsev. Resistive forces in swimming. In V. Zatsiorsky, editor, *Biomechanics in Sports: Performance Enhancement and Injury Prevention*, volume 9 of *Encyclopedia of Sport Medicine.*, chapter 5. Blackwell, IOC Medical Commission, 2000.

[5] H. Takagi, Y. Shimizu, and N. Kodan. A hydrodynamic study of active drag in swimming. *JSME International Journal Series B*, 42(2):171–177, 1999. doi: 10.1299/jsmeb.42.171.

[6] J. van Houwelingen, S. Schreven, J.B.J. Smeets, H.J.H. Clercx, and P.J. Beek. Effective propulsion in swimming: Grasping the hydrodynamics of hand and arm movements. *Journal of Applied Biomechanics*, 33(1):87–100, 2017. doi: 10.1123/jab.2016-0064.

[7] A.D. Lyttle, B.A. Blanksby, B.C. Elliott, and D.G. Lloyd. Net forces during tethered simulation of underwater streamlined gliding and kicking techniques of the freestyle turn. *Journal of Sports Sciences*, 18(10):801–807, 2000. doi: 10.1080/026404100419856.

[8] P.K. Kundu and I.M. Cohen. *Fluid Mechanics, Second Edition.* Academic Press, 2001. ISBN 0121782514.

[9] G.J.F. van Heijst. *Geophysical Fluid Dynamics. Lecture notes.* Fluid Dynamics Laboratory, Eindhoven, 2004.

[10] M. van Dyke. *Perturbation Methods in Fluid Mechanics.* Parabolic Press, Stanford, 1975.

[11] R. Arellano, S. Pardillo, and A. Gavilán. Usefulness of strouhal number in evaluating human under-water undulatory swimming. 2003.

[12] (awaiting approval) J. van Houwelingen, R.M. Antwerpen, A.P.C. Holten, E.J. Grift, J. Westerweel, and H.J.H. Clercx. Automated LED tracking to measure instantaneous velocities in swimming. *Sports Engineering.*